Electronic Supplementary Information

Table S1. Selected crystal data and structure refinement for **1** and **2**

	1	**2**
Chemical formula	$C_9H_{33.5}GdN_{15}O_{13.75}$	$C_9H_{36}N_{15}O_{15}Y$
M_r	729.26	683.44
Crystal system	orthorombic	orthorombic
T / K	293	293
a, b, c (Å)	21.305(5), 6.840(2), 18.770(5)	14.277 (4), 16.767 (5), 11.966 (5)
V (Å^3)	2735.08 (13)	2864.20 (17)
Z	4	4
M / mm^{-1}	2.52	2.12
Crystal size / mm	0.19x0.16x0.11	0.43x0.33x0.20
No. of measured, independent and observed [I>2σ(I)] reflections	23963, 4911, 3854	11130, 3257, 1842
R_{int}	0.069	0.059
(sin θ/λ)$_{max}$ (Å^{-1})	0.650	0.0650
$R[F^2 > 2\sigma(F^2)]$, $wR(F^2)$, S	0.037, 0.087, 1.02	0.043, 0.092, 1.01
No. of reflections	4911	3257
No. of parameters	380	192
$\Delta\rho_{max}$, $\Delta\rho_{min}$ (e Å^{-3})	1.31,–1.18	0.40, –0.88

Table S2. C-O bonds lengths (Å) and O-C-O angles (^{o}) in **1** and **2**

Bond lenghts / Å			angles / ^{o}	
		1		
C1-O13	1.255(13)		O13-C1-O12	122.2(13)
C1-O12	1.270(14)		O13-C1-O11	120.5(12)
C1-O11	1.304(14)		O12-C1-O11	117.3(9)
C2-O22	1.270(16)		O22-C2-O23	122.9(14)
C2-O23	1.263(18)		O22-C2-O21	117.6(12)
C2-O21	1.305(16)		O23-C2-O21	119.5 (14)
C3-O32	1.280(17)		O32-C3-O33	122.2(13)
C3-O33	1.282(14)		O32-C3-O31	121.4(12)
C3-O31	1.301(15)		O33-C3-O31	116.4(12)
C4-O42	1.261(12)		O42-C4-O41	120.4(8)
C4-O41	1.291(12)		O42-C4-O43	122.4(8)
C4-O43	1.283(11)		O41-C4-O43	117.2(9)
		2		
C1-O3	1.266(4)		O3-C1-O1	122.5(3)
C1-O1	1.287(3)		O3-C1-O2	121.7(3)
C1-O2	1.299(3)		O1-C1-O2	115.9(3)
C2-O5	1.249(4)		O5-C2-O6	123.3(3)
C2-O6	1.295(3)		O5-C2-O4	122.1(3)
C2-O4	1.306(3)		O6-C2-O4	114.6(3)

Section S1 – Group theory.

The approximate point symmetry of the $[Gd(CO_3)_4(H_2O)]^{5-}$ complex in **1** is ~C_4, whill the $[Y(CO_3)_4]^{5-}$complexes in **2** has a D_{2d} point symmetry. We assume that Eu^{3+} or Cm^{3+} in the doped compounds also adopt these symmetries. We applied group theory to obtain the number of spectral lines for the $^7F_0$ ✂ $^{2S+1}L_J$ and $^5D_0$ ✂ ^7F_J transitions in the UV-vis spectra of Eu^{3+} doped in **1** and **2** (UV-vis spectra are shown in Fig. 2). The results are listed in Tables 1A and 2A.

Table S3. Number of observed and predicted spectral lines of the $[Eu(CO_3)_4(H_2O)]^{5-}$ complex in **1**. The observed spectral lines are from the UV-vis absorption spectra (cf. Fig. 2) while the predicted, theoretical lines are from group theory with C_4 point symmetry.

$J_{0\text{-}4}$	Decomposition into irreducible representation	predicted spectral lines	observed spectral lines
0	A	1	1
1	A+E	2	2
2	A+2·B+E	2	2
3	A+2·B+2·E	3	1
4	3·A+2·B+2·E	5	5

Table S4. Number of observed and predicted spectral lines of the $[Eu(CO_3)_4]^{5-}$ complex in **2**. The observed lines are from the UV-vis absorption spectra (cf. Fig. 2) and the predicted, theoretical lines from group theory with D_{2d} point symmetry.

$J_{0\text{-}4}$	Decomposition into irreducible representation	predicted spectral lines	observed spectral lines
0	A_1	0	1
1	A_2+E	1	2
2	A_1+B_1+B_2+E	2	3
3	A_2+B_1+B_2+2·E	3	3
4	2·A_1+A_2+B_1+B_2+2·E	3	3

Table S5. Parameters values used in calculations used in Pitzer model

Parameter
$\Delta H^o = 31.4\ \mathrm{kJ \cdot mol^{-1}}$
$\beta^0_{K-[Eu(CO_3)_3^{3-}]} \in (0.001;0.85)$
$\beta^0_{K-[Eu(CO_3)_4^{5-}]} \in (3.7;6.5)$
$\beta^1_{K-[Eu(CO_3)_3^{3-}]} \in (1;2.1)$
$\beta^1_{K-[Eu(CO_3)_4^{5-}]} \in (19;24)$
$\Psi_{K-[Eu(CO_3)_n^{-2n+3}]} = 0$
$\theta_{K-[Eu(CO_3)_n^{-2n+3}]} = 0$

Section S2 – IR spectra of solid state and solutions.

IR spectra of solid state. The IR spectra of the rare earth tetracarbonates, as well as $[C(NH_2)_3]_2CO_3$ were recorded in the range of 50 to 4000 cm^{-1} at room temperature. The assignment of the appropriate internal modes of compounds under study, following M. Dahm et al ,[1] and Janicki et al [2] are presented in Figure S1.

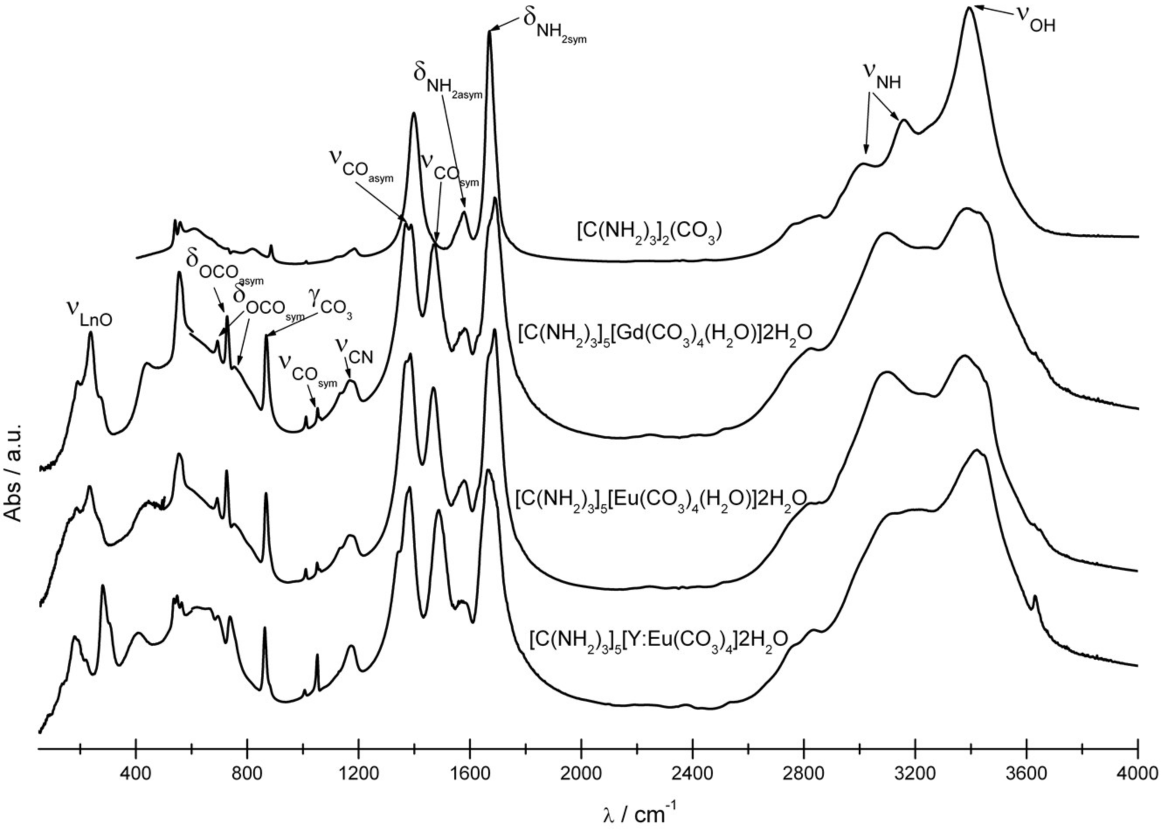

Figure S1. IR spectra of compounds under study.

The changes in the nearest surrounding of the Ln^{3+} ion are reflected in the variation of the bands that were observed in the spectral range of 220 to 320 cm^{-1}. The bands located between in this range may be attributed to the ν_{Ln-O} vibrations. The group of sharp bands centered at ~685, 725, 750cm^{-1} are attributed to the δ_{OCO} vibrations while the band at ~860 cm^{-1} is assigned as γ_{CO3} . The other group of bands connected with CO_3^{2-} vibrations are located at 1060 cm^{-1} (ν_{OCOsym} and $\nu_{OCOasym}$) as well as 1375 cm^{-1} and 1470 cm^{-1} – $\nu_{OCOasym}$ and ν_{OCOsym}, respectively. The strong and sharp bands that were found in the region of 1640 to 1720 cm^{-1} were assigned to the δ_{HNH} and δ_{HOH} vibrations. The most intense, wide bands that are located in the spectral range between 2500 and 3750 cm^{-1} are attributed to the ν_{NH} and ν_{OH} oscillations and to the $2\nu_{CO}$, $2\delta_{HNH}$, and $2\delta_{HOH}$ overtones.[2]

IR spectra of solutions. The IR spectra of the lanthanide carbonate solutions were measured in the spectral range of 1000 to 4000 cm^{-1}. The bands of the ν_{CO} (1300–1550 cm^{-1}) and δ_{OH2} (1600–1750 cm^{-1}) vibrations in the Y(III)-carbonate and Eu(III)-carbonate complexes in solution spectra, as well as those of H_2O and K_2CO_3, are shown in Figure S2. The spectra of the appropriate crystals **1** and **2** are also included for comparison purposes. The peak at

1393 cm^{-1} in the spectra of the solutions and K_2CO_3 solutions was attributed to the uncomplexed carbonate anion. This band partially obscures the bands at 1373 cm^{-1} (ν_{COasym}) and 1462 cm^{-1} (ν_{COsym}) from the coordinated carbonate anions in the Eu(III)-carbonate complex in solution. Better resolved spectra were recorded in the case of the Y(III)-carbonate complexes in solution. The shoulder at 1462 cm^{-1} and the peak at 1485 cm^{-1} that were observed in the spectra of the Eu(III) and Y(III) solutions, respectively, are assigned to the ν_{CO} vibrations of C–O bonds from the complexed CO_3^{2-} anion. As previously shown,[14][2]the difference between the band positions in the spectra of **1** (at ca. 1460 cm^{-1}) and **2** (at ca. 1490 cm^{-1}) may be an indication of the change in the coordination number of M^{3+} in tetracarbonate complex.

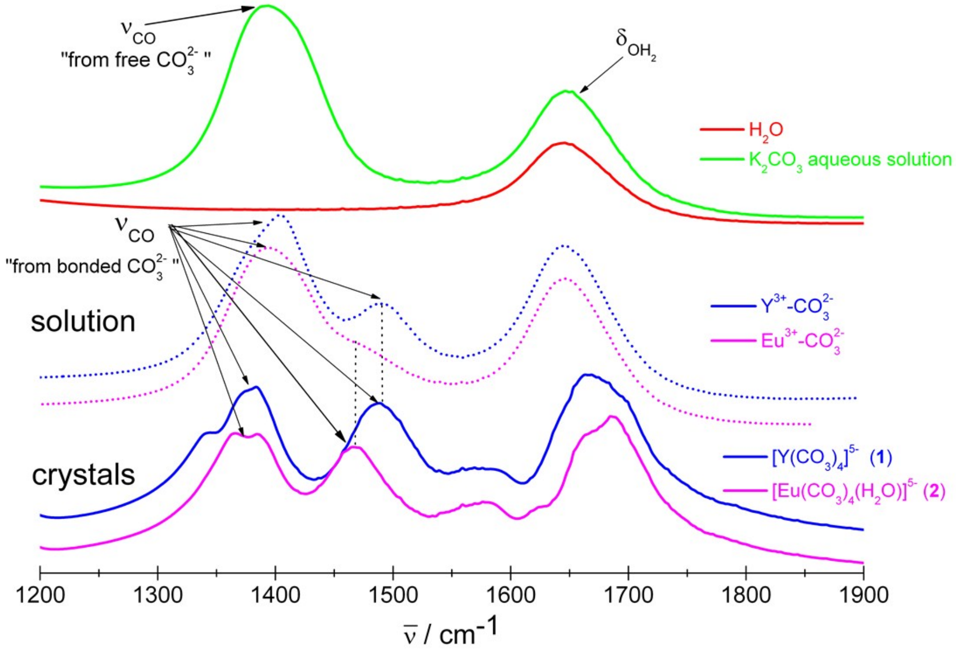

Figure S2. IR spectra of Y^{3+}–CO_3^{2-}, Eu^{3+}–CO_3^{2-} solutions as well as crystals **1** and **2**.

References:
[1] M. Dahm, and A. Adam, *Z. Anorg. Allg. Chem.*, 2001, **627**, 2023-2031.
[2] R. Janicki, P. Starynowicz and A. Mondry, *Eur. J. Inorg. Chem.,* 2011, 3601-3616.

Section S3 – Stretching f_{MO} force constants and nature of Ln-O bond

The Raman and IR spectra of **1** and **2** measured in the spectral region 100–400 cm^{-1} are presented in Figure S3.

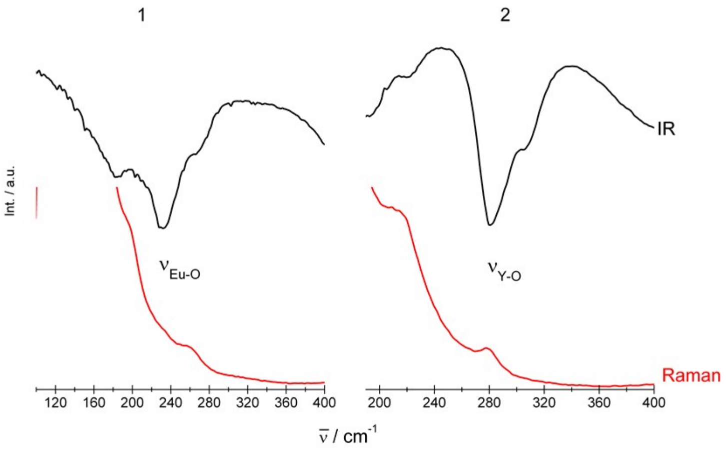

Figure S3. IR (black) and Raman (red) spectra of **1** and **2**.

The band centered at 280 cm^{-1} in the spectrum of 2 is sharp and well resolved while in the spectrum of 1 only a shoulder at ~235 cm^{-1} is observed. Although it is difficult to compare the intensity of bands in the Raman spectra of different systems, analysis of the intensity ratios of relevant bands for different spectra may provide useful information about nature of the discussed bonds. According to this the intensity of $\nu_{Y\text{-}O}$ bands seems to be a little bit more intense than $\nu_{Gd\text{-}O}$. As the appearance of a vibrational Raman band arises from a change in bond polarisability with variation of bond lengths during oscillation, the presence of better resolved band in the spectrum of 2 may reflect a certain degree electron sharing in the M^{3+}–$O(CO_3^{2-})$ interaction. Because the nature of bond is in a way reflected in stretching force constant, it is worth to consider the changes of this spectroscopic factor in the series of lanthanide ions. We have decided to calculate the force constants of stretching $\nu_{Ln\text{-}O}$ vibration using a simple relationship:

$$f_{MO} = (\nu_{MO}{}^2\mu_{MO}/\nu_{ScO}{}^2\mu_{ScO})\cdot f_{ScO}$$

where: f is stretching force constant, ν is wavenumber of stretching vibration, μ is reduced mass of diatomic oscillator. For these calculations we have used the ab initio theoretical results for isostructural $[Sc(CO_3)_4]^{5-}$ anion (f_{ScO}=1.758 mDyn·Å^{-1} and ν_{ScO}=309 cm^{-1}) as a reference data.[1] We are aware of the limitation of such data, which base on a rough approach of the simple diatomic oscillator model. However our intension was not to find accurate values of stretching f_{MO} force constants, but to show the trend of changes of this parameter across lanthanide tetracarbonate series. The changes of f_{MO} as a plot of M-O bond lengths are presented in Figure S4.

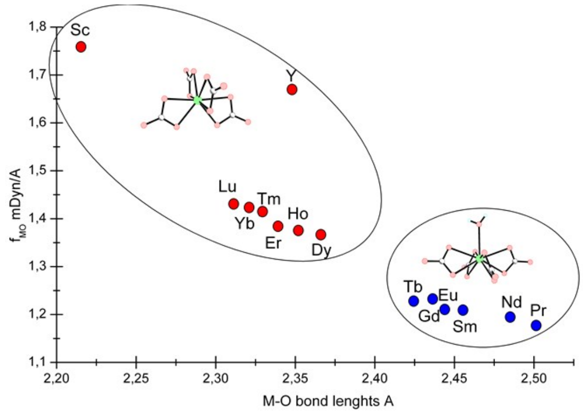

Figure S4. The changes of f_{MO} stretching force constants as a function of M-O bond lengths for compounds under study.

Interestingly the calculated values of $f_{Ln\text{-}O}$ are comparable to those determined from force field analysis of the $[Ln(DMSO)_8]I_3$ systems (where DMSO is dimethylsulfoxide).[2] As it is seen form Figure S4 the stretching force constant values monotonically increase with shortening of M-O bond lengths in the series of isostructural tetracarbonate complexes. In general the force constants values of eight coordinate $[Ln(CO_3)_4]^{5-}$ complexes are smaller than those for nine-coordinate $[Ln(CO_3)_4(H_2O)]^{5-}$ complexes. The $f_{Sc\text{-}O}$ and $f_{Y\text{-}O}$ values significantly deviate from the others. These results seem to confirm the conclusion, as degree of covalence in Ln-O bond in the series of lanthanide complexes increase with atomic number. Consequently the Sc-O and Y-O interaction should be more covalent in comparison with the Ln-O ones.

It was shown by us previously that in description of typically ionic Lu-O interaction in $[Lu(CO_3)_4]^{5-}$ complex its partial covalent character should be considered. This covalent (~10%) interaction may be describe as donation of electron density from $sp^{3.7}$ orbitals of oxygen atom to the empty hybridized $6s6p^{0.8}5d^{4.1}$ orbital of Lu^{3+}.[3] It should be noted that 4f electrons of Lu^{3+} are completely nonbonding within this model. Thus the question arises how “covalent contribution” to the Ln–O bond reflects in the unusual intensity of hypersensitive f-f transitions. According to Judd and Ofelt theory the intensity of f-f transitions is a consequence of mixing of states of opposite parity manifested here, by admixture of d (hybridized $6s6p^{0.8}5d^{4.1}$) and 4f orbitals of Ln^{3+}. Consequently the contribution of covalent bond to the substantially ionic Ln–O interaction may disturb intensity of f-f- transitions.

An increase of covalence contribution with atomic number is probably an additional factor stabilizing formation of highly negative tetracarbonate complexes of heavier lanthanides in comparison with the lighter one.

[1] M. Dahm, and A. Adam, *Z. Anorg. Allg. Chem.*, 2001, **627**, 2023-2031.

[2] A. Abbasi, E. D. Risberg, L. Eriksson, J. Mink, I. Persson, M. Sandström, Y. V. Sidorov, M. Y. Skripkin, A. S. Ullström, *Inorg. Chem.,* 2007, **46**, 7731-7741.

[3] R. Janicki, P. Starynowicz and A. Mondry, *Eur. J. Inorg. Chem.,* 2011, 3601-3616.

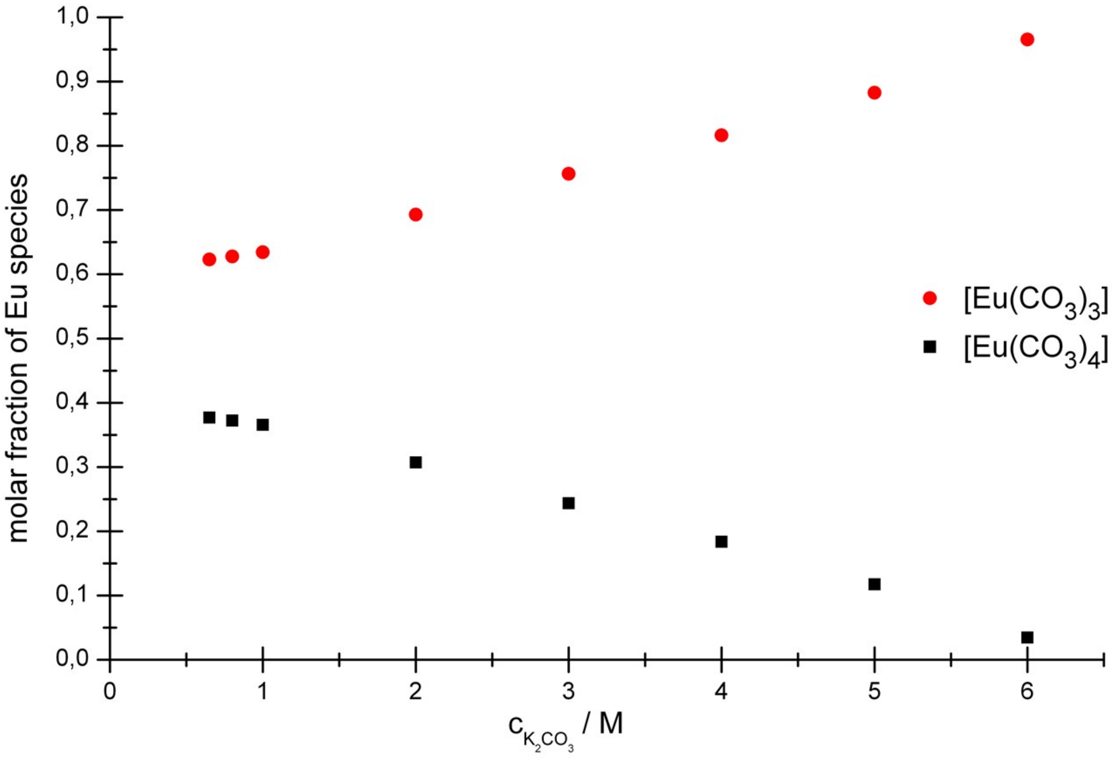

Figure S5. Molar fraction of $[Eu(CO_3)_n]$ species as a function of K_2CO_3 concentration.

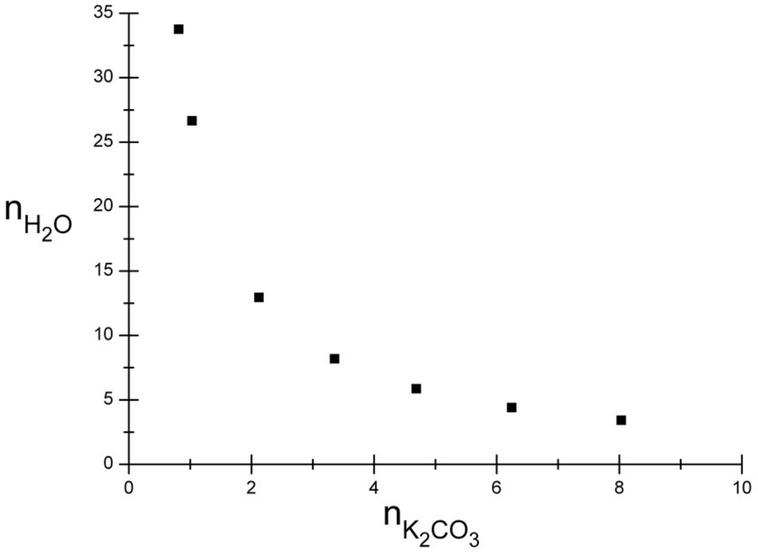

Figure S6. The number of H_2O moles per K_2CO_3 moles in aqueous solutions of K_2CO_3.

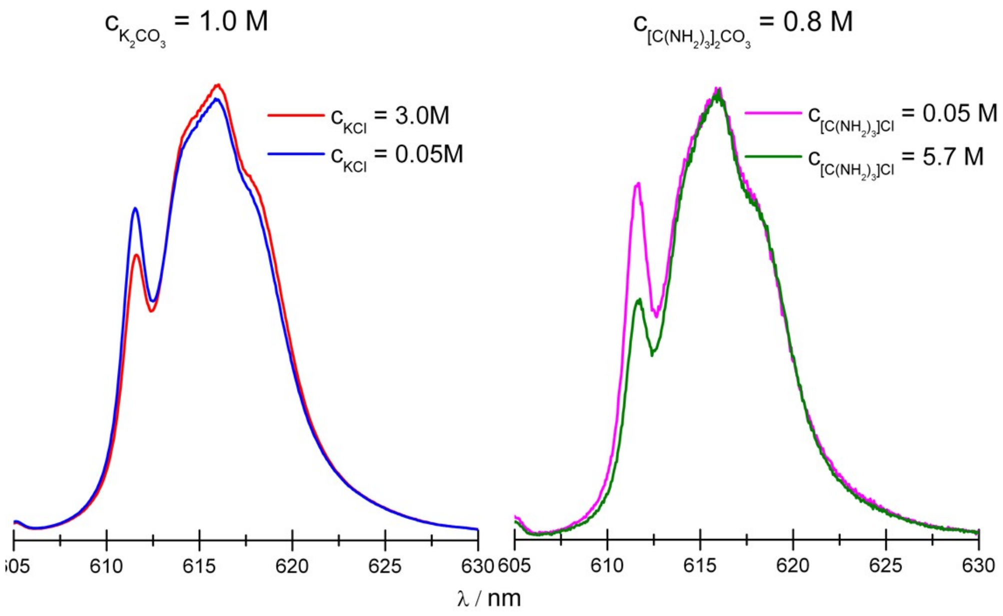

Figure S7. The luminescence spectra of the hypersensitive $^5D_0 \rightarrow {}^7F_2$ transition of $EuCl_3$–K_2CO_3–KCl and $EuCl_3$–$[C(NH_2)_3]_2CO_3$–$[C(NH_2)_3]Cl$ aqueous solutions at different concentration of KCl/$[C(NH_2)_3]Cl$ medium.

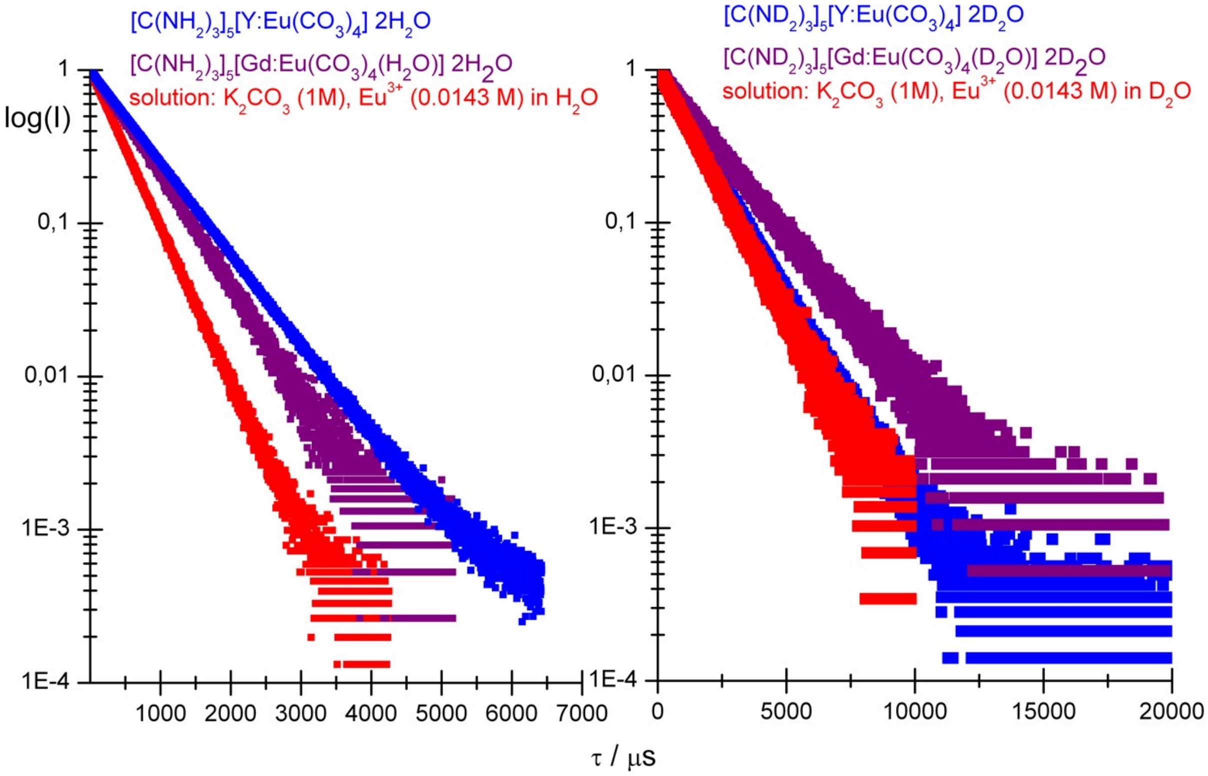

Figure S8. The luminescence lifetimes of the $^5D_0$ state for compounds under study in H_2O and in D_2O.

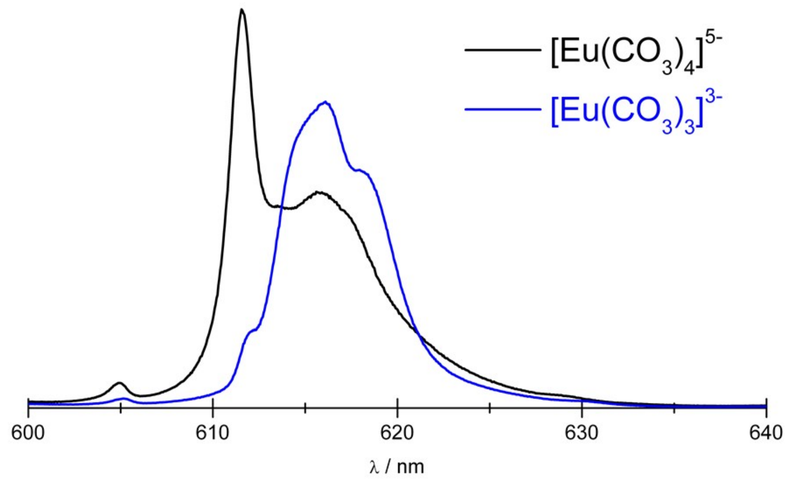

Figure S9. The luminescence spectra of the hypersensitive $^5D_0$ → $^7F_2$ transition of pure $[Eu(CO_3)_4]^{5-}$ and $[Eu(CO_3)_3]^{3-}$ species in solution.

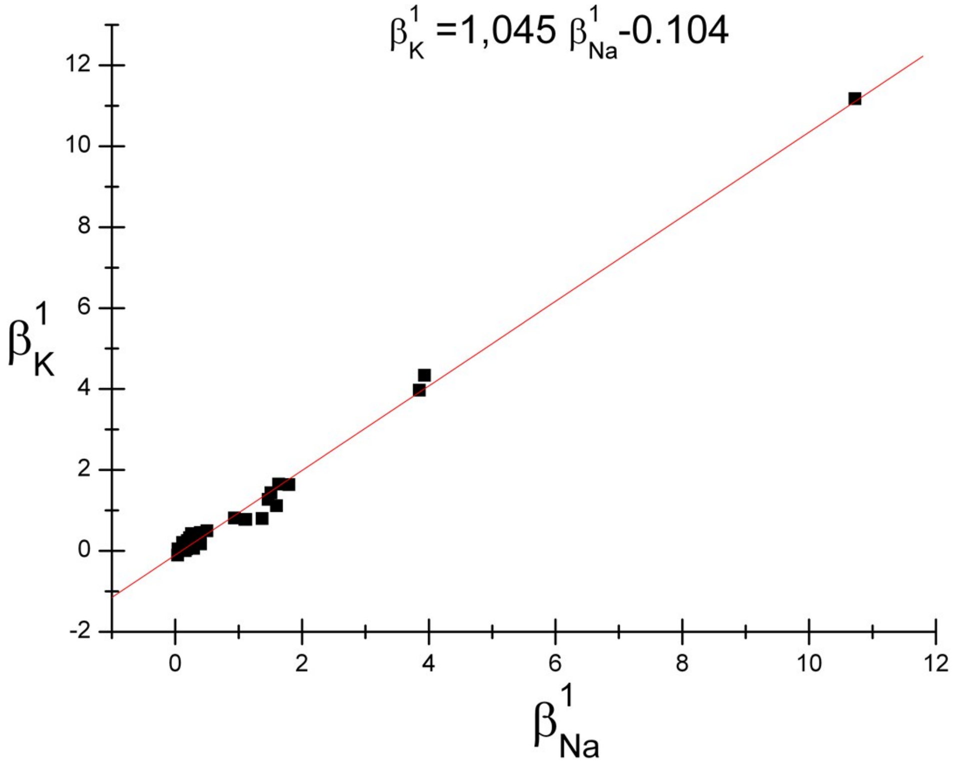

Figure S10. The plot of β_K^1 versus β_{Na}^1. The data were taken from [39] and [52].